
PICTORIAL ESSAY

Magnetic Resonance Imaging of Prostate Cancer

KYK Wong, CYH Chan, KY Kwok, WK Wong, KW Tang

Department of Radiology and Imaging, Queen Elizabeth Hospital, Hong Kong

ABSTRACT

Prostate cancer is a common entity in elderly men. Diagnosis is based on histology obtained from transrectal ultrasound-guided biopsies, whereas magnetic resonance (MR) imaging can be used for local staging of prostate cancer. MR features of extracapsular extension are particularly important as it leads to upstaging of the tumour and significantly affects both treatment and prognosis. The purpose of this review was to demonstrate the MR imaging appearance of different stages of prostate cancer. MR spectroscopy can also aid in improving the diagnosis. Accurate staging can ensure appropriate management and prevent recurrence due to inadequate treatment.

Key Words: Diffusion magnetic resonance imaging; Magnetic resonance imaging; Prostate neoplasms

中文摘要

前列腺癌的磁共振成像

黃汝麒、陳彥豪、郭啟欣、王旺根、鄧國穎

前列腺癌是老年男性常見的疾病。診斷前列腺癌可經直腸超聲引導的活檢而獲得組織作化驗，而磁共振（MR）成像可用於前列腺癌的局部分期。MR特徵有助了解前列腺癌是否有外擴散的跡象，這點相當重要，因為外擴散會導致腫瘤評分升級，並會影響治療和預後。本文探討前列腺癌不同階段的MR成像。MR波譜有助於診斷。準確的分期對於確保適當的治療有重要意義，從而防止因治療不徹底而造成復發。

INTRODUCTION

Prostate cancer is common among the Hong Kong male population, with an incidence of 28.5 per 100,000 in 2012. Prostate cancer is the third most common malignancy and is the fifth major cause of cancer deaths in Hong Kong.¹ Both the incidence rate and crude mortality have been steadily increasing over the past decade. Management mainly consists of watchful

waiting, radical prostatectomy, hormonal therapy, or radiotherapy.² The choice of management pathway depends on a number of factors, including patient age, premorbid status, prostate-specific antigen levels, and the stage of disease. Pretreatment magnetic resonance imaging (MRI) of the prostate plays a crucial role in local staging of the disease, as well as predicting extracapsular extension (ECE) at final pathology.^{3,4}

*Correspondence: Dr Kevin YK Wong, Department of Radiology and Imaging, Queen Elizabeth Hospital, 30 Gascoigne Road, Jordan, Kowloon, Hong Kong.
Email: kevirgwong@gmail.com*

Submitted: 15 Jan 2015; Accepted: 9 Mar 2015.

Detection of ECE on MRI carries a high risk of subsequent biochemical failure and may alter treatment from curative surgery to non-surgical treatment. Recent studies have shown high sensitivity and specificity for ECE and seminal vesicle invasion of MRI.^{5,6}

PROSTATIC ANATOMY

The prostate gland is an inverted pyramid-shaped structure situated just inferior to the urinary bladder. The prostate gland completely surrounds the prostatic urethra as it exits the bladder base and traverses the prostate gland in its anterior portion. The zonal anatomy of the prostate was first described by McNeal⁷ according to function and histology. The prostate gland is divided into four distinct zones: the peripheral zone (constituting 70% of the gland), central zone (constituting 20% of the gland), transition zone (constituting 5% of the gland), and anterior fibromuscular zone (constituting 5% of the gland). The peripheral zone is the most common site for development of prostate cancer and is posterolateral in location. The central zone is the region surrounding the ejaculatory ducts and is located at the bladder base. The transition zone is the tissue immediately surrounding the prostatic urethra proximal to the verumontanum and is the most common location for benign prostatic hyperplasia. The anterior fibromuscular stroma does not contain glandular tissue and consists of fibrous and muscular components.

MAGNETIC RESONANCE IMAGING TECHNIQUES AND SEQUENCES

Several MRI sequences are currently available for prostate imaging, including standard T1- and T2-weighted images, diffusion-weighted imaging (DWI), dynamic contrast-enhanced imaging (DCE-MRI), and MR spectroscopy (MRS). T1-weighted large field of view (FOV) imaging allows an overview of the pelvic anatomy, and detection of post-biopsy haemorrhage and extra-prostatic disease, including nodal and osseous metastasis. T2-weighted imaging with small FOV in thin sections allows tumour detection, localisation, and staging. DWI offers a second parameter to increase the sensitivity and specificity of detection and offers an increased detection rate when combined with T2-weighted imaging.^{8,9} Contrast-enhanced MRI is another adjunct to conventional MRI, which increases the detection rate and is considered optional.¹⁰

At 1.5 T, MRI of the prostate can make use of both the endorectal and pelvic coil. The pelvic coil provides a larger FOV for detection of nodal and osseous

metastasis. The endorectal coil provides a smaller FOV, thus increasing the signal-to-noise ratio and spatial resolution¹¹ for better cancer delineation. At 3 T, the signal-to-noise ratio is increased¹² and the use of the endorectal coil has not been determined, so the use of the pelvic coil alone may save time and reduce patient discomfort.¹³

At Queen Elizabeth Hospital in Hong Kong, almost all patients undergoing MRI of the prostate have biopsy-proven prostate cancer, either done by transrectal ultrasound (TRUS)-guided biopsy or by transurethral resection of prostate, as we do not offer screening or primary tumour detection of carcinoma of the prostate gland by MRI. Thus, the main purposes of imaging are for staging and detection of ECE. The standard imaging sequences include conventional large FOV T1-weighted images in the axial plane, small FOV T2-weighted images in three orthogonal planes, DWI and a 1-mm thin-slice T2-weighted three-dimensional SPACE (Sampling Perfection with Application optimized Contrasts using different flip angle Evolution) axial image.

Post-biopsy haemorrhage is a factor affecting the timing of post-biopsy MRI. Blood in the peripheral zone can be hypointense on T2-weighted images, which would obscure underlying prostate cancer and affect the accuracy of MRI in lesion detection. The current recommendation is to wait 4 to 6 weeks to perform post-biopsy MRI to allow adequate time for resolution of any haemorrhage.^{14,15}

Magnetic Resonance Imaging Appearance of the Prostate and Periprostatic Anatomy

Conventional T1- and T2-weighted imaging sequences are used to evaluate gross pelvic anatomy and prostatic anatomy, respectively. On T1-weighted images, the prostate demonstrates low-to-intermediate signal intensity, while the zonal anatomy is not well delineated due to insufficient tissue contrast resolution between zones. T2-weighted images are most ideal for zonal anatomy depiction.

On T2-weighted images, the central and transition zones have similar low-to-intermediate signal intensity. Differentiation may not be possible, but is rarely important, as the purpose of imaging is to detect ECE. The peripheral zone appears as a relatively hyperintense crescent of tissue covering the posterolateral regions of the prostate. A thin hypointense rim of tissue

representing the anatomical prostatic capsule surrounds the peripheral zone. The seminal vesicles appear as high signal intensity, elongated, convoluted structures on both sides posterior to the prostate gland. The neurovascular bundles are located posterolateral to both sides of the prostate and are represented by low-intensity 'dot-like' structures (Figure 1). For the purpose of describing lesion location, the prostate can be divided into six sections based on thirds in a cranio-caudal direction (base, mid-gland, and apex) and then left and right sides.

Magnetic Resonance Imaging Appearance of Localised Prostate Cancer

Prostate cancer can be anatomically staged using Union for International Cancer Control TNM staging¹⁶ (Table 1). By definition, T0 and T1 tumours are not visible on imaging and are detected clinically or with TRUS-guided biopsy. Localised prostatic tumours fall into the T2 category. This can be further subdivided into T2a, T2b, and T2c based on the extent of involvement within the prostate gland.

On T1-weighted images, prostate cancer appears as low-

intensity lesions against a homogeneous low-intensity prostate gland. Thus, lesion detection is difficult. On T2-weighted images, prostate cancer appears as low-intensity lesions in the high-signal-intensity peripheral zone. This offers the best tissue contrast for anatomical detection (Figure 2). Differential diagnosis of a low-signal-intensity lesion on T2-weighted images includes post-biopsy haemorrhage, benign prostatic hyperplasia changes or may be due to previous radiotherapy or hormonal therapy.

On DWI, prostate cancer appears as an area of restricted diffusion showing high intensity on DWI and reduced intensity on the apparent diffusion coefficient map. Different *b* values exist for DWI of the prostate from *b*=0 to *b*=1000 s/mm². *b*=1000 s/mm² has been shown to offer optimal sensitivity for lesion detection.¹⁷ At Queen Elizabeth Hospital, we use *b*=0, 50, 500, and 1000 s/mm² for most prostate imaging.

Post-biopsy haemorrhage usually appears as high signal intensity on T1-weighted images and low signal intensity on T2-weighted images (Figure 3). It is recommended to wait 4 to 6 weeks after TRUS-guided

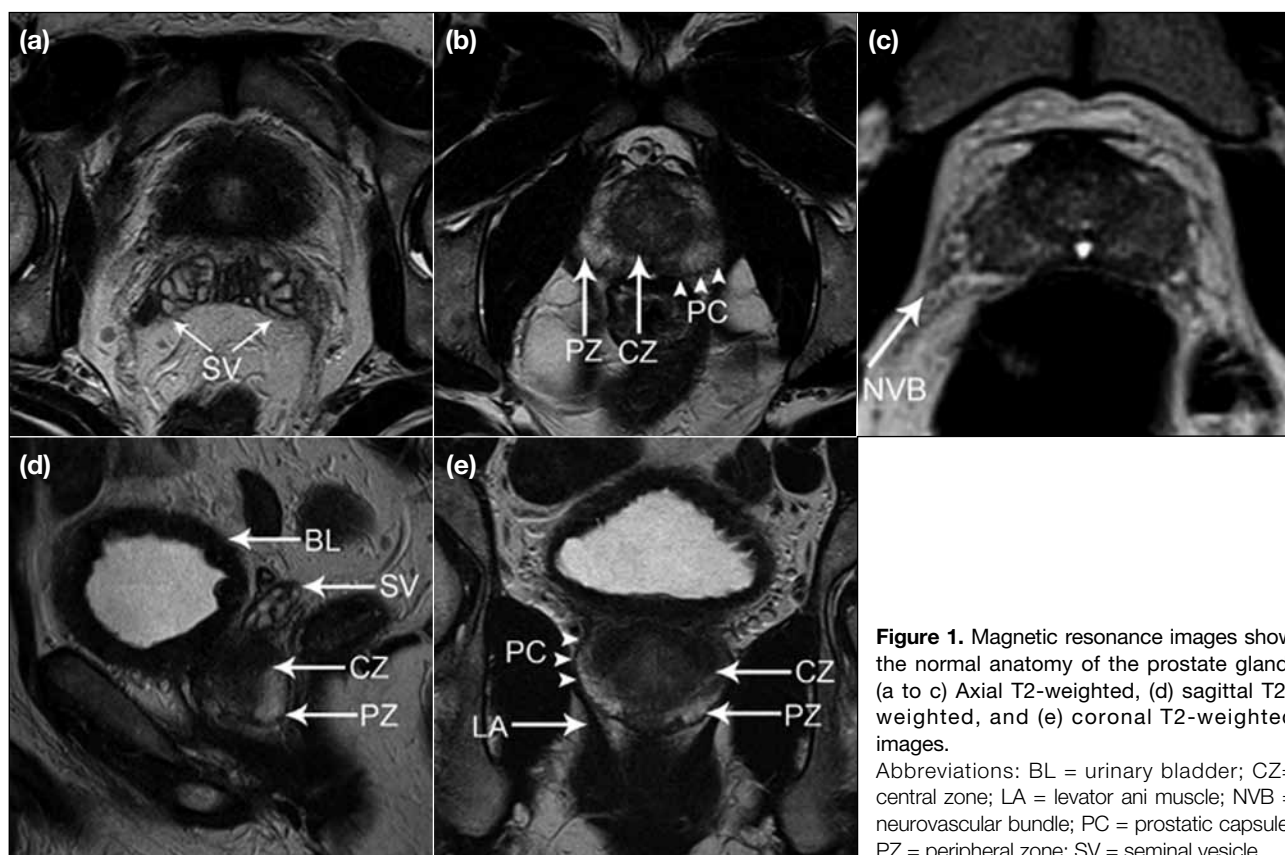


Figure 1. Magnetic resonance images show the normal anatomy of the prostate gland. (a to c) Axial T2-weighted, (d) sagittal T2-weighted, and (e) coronal T2-weighted images. Abbreviations: BL = urinary bladder; CZ = central zone; LA = levator ani muscle; NVB = neurovascular bundle; PC = prostatic capsule; PZ = peripheral zone; SV = seminal vesicle.

Table 1. Union for International Cancer Control clinical staging of prostate cancer.

Staging	Description
Tumour staging (T)	
TX	Primary tumour cannot be assessed
T0	No evidence of primary tumour
T1	Clinically inapparent tumour neither palpable nor visible by imaging
T1a	Tumour incidentally found on histology in $\leq 5\%$ of resected tissue
T1b	Tumour incidentally found on histology in $\geq 5\%$ of resected tissue
T1c	Tumour identified on needle biopsy
T2	Tumour confined within prostate
T2a	Tumour involving $\frac{1}{2}$ of one lobe or less
T2b	Tumour involving more than $\frac{1}{2}$ of one lobe but not both lobes
T2c	Tumour involving both lobes
T3	Tumour extending through the prostate capsule
T3a	Extracapsular extension
T3b	Seminal vesicle(s) invasion
T4	Tumour is fixed or invades adjacent structures other than seminal vesicles, such as external sphincter, rectum, bladder, levator muscles, and/or pelvic wall
Nodal staging (N)	
NX	Regional lymph nodes not assessed
N0	No regional lymph node metastasis
N1	Metastasis in regional lymph node(s)
Metastasis staging (M)	
M0	No distant metastasis
M1	Distant metastasis
M1a	Non-regional lymph node(s)
M1b	Bone(s)
M1c	Other sites with or without bone disease

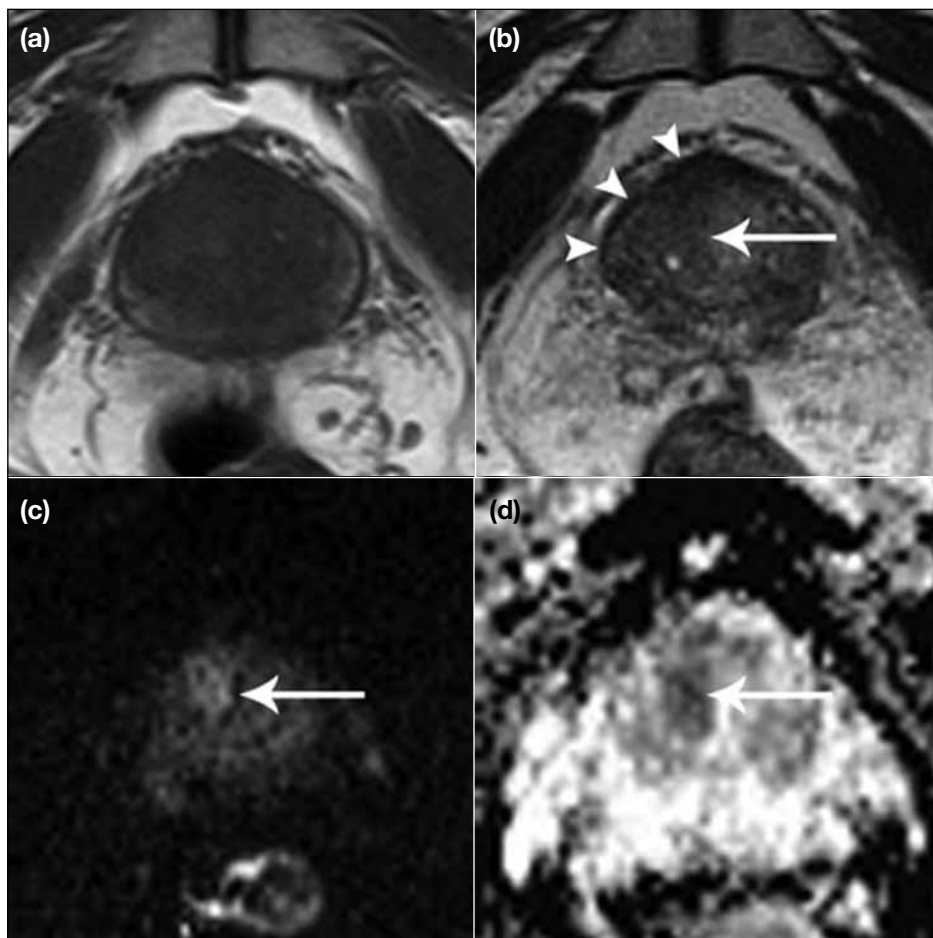


Figure 2. Magnetic resonance images of a 60-year-old man with biopsy-proven prostatic adenocarcinoma. (a) Axial T1-weighted image shows the tumour is not apparent as both the tumour and normal prostate tissue shows low signal intensity. (b) Axial T2-weighted image shows the tumour clearly delineated as a low-signal-intensity lesion in the right anterior peripheral and central zone (arrow). The overlying T2-weighted low-signal rim representing the prostatic capsule is intact (arrowheads). (c and d) Axial diffusion-weighted image and corresponding apparent diffusion coefficient map show restricted diffusion demonstrated by the tumour ($b = 1000 \text{ s/mm}^2$) [arrows].

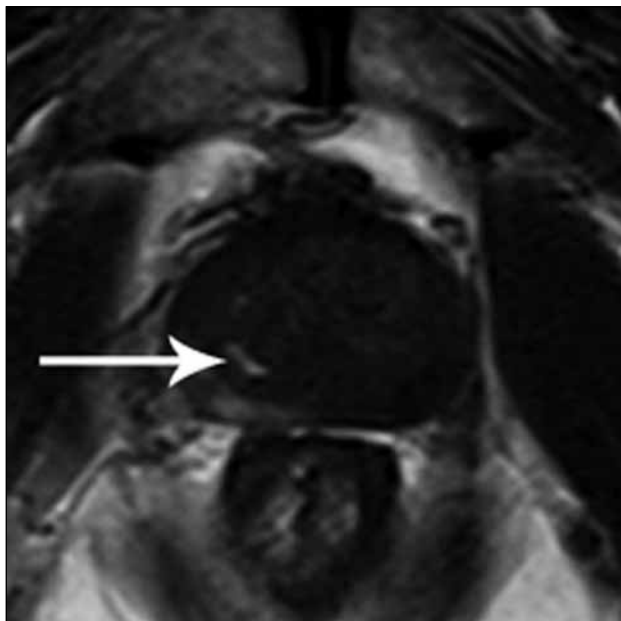


Figure 3. Magnetic resonance image shows post-biopsy haemorrhage. Axial T1-weighted image of the prostate gland for suspected malignancy demonstrates T1 high signal intensity within the right side of the prostate gland (arrow) signifying blood.

biopsy to prevent artefacts caused by biopsy-related haemorrhage.¹⁸

Magnetic Resonance Imaging Features of Extracapsular Extension

Tumours that have infiltrated beyond the anatomical capsule of the prostate are defined as T3 disease. The category is subdivided into T3a (ECE) and T3b (seminal vesicle invasion). T4 disease denotes invasion into adjacent structures other than the seminal vesicles, including the external sphincter, rectum, urinary bladder, levator ani muscles, or pelvic sidewalls.

Several features are used to define ECE (Table 2), and recent guidelines from the European Society of Urogenital Radiology have suggested a 5-point scale to assess the probability of ECE based on imaging findings, which gives a score to different features of ECE — higher score denotes a higher probability of ECE in the Prostate Imaging – Reporting and Data System (Table 3).¹⁸ Diagnosis of ECE is important due to its implications for treatment. The presence or absence of ECE would influence the plan of management by radical prostatectomy or radiotherapy. However, when the disease reaches T3, radical prostatectomy alone is associated with a high risk of positive resection margins

Table 2. Features of extracapsular extension on magnetic resonance imaging.

Abutment, irregularity, or interruption of the anatomical capsule by tumour
Obliteration of the rectoprostatic angle
Encasement or thickening of the neurovascular bundle
Seminal vesicle(s) invasion
Focal bulging of mass

Table 3. European Society of Urogenital Radiology scoring system for extracapsular extension.¹⁸

Criteria	Findings	Score
Extracapsular extension	Abutment	1
	Irregularity	3
	Neurovascular bundle thickening	4
	Bulge, loss of capsule	4
	Measurable extracapsular disease	5

and positive lymph nodes and increased risk of local or nodal recurrence. Thus, radiotherapy or hormonal therapy, either as adjuvant or salvage therapy, may be indicated for stage T3 disease¹⁹ (Figures 4 to 8).

Magnetic Resonance Imaging Features of Metastatic Disease

Common sites of distant metastasis of carcinoma of the prostate include bone, lymph nodes, lung, liver, and brain. On MRI, large FOV T1-weighted images provide the best coverage of the pelvis to detect osseous and nodal metastasis.

Normal bone marrow in elderly men usually undergoes fatty marrow replacement and demonstrates high signal intensity on T1-weighted imaging. The bony cortex is dense calcium so it shows up as low-intensity cortices. Metastatic prostate cancer usually demonstrates T1-weighted low signal and gives excellent tissue contrast compared with the surrounding healthy bone marrow (Figure 9).

Enlarged lymph nodes also demonstrate T1-weighted low signal against the background of high-signal pelvic fat. Nodal metastases can spread to the obturator, hypogastric, external iliac, internal iliac, common iliac, and para-aortic nodes (Figure 10).²⁰ Metastases to other regions of the body are uncommon, but can include adrenal glands, spleen, or peritoneum.

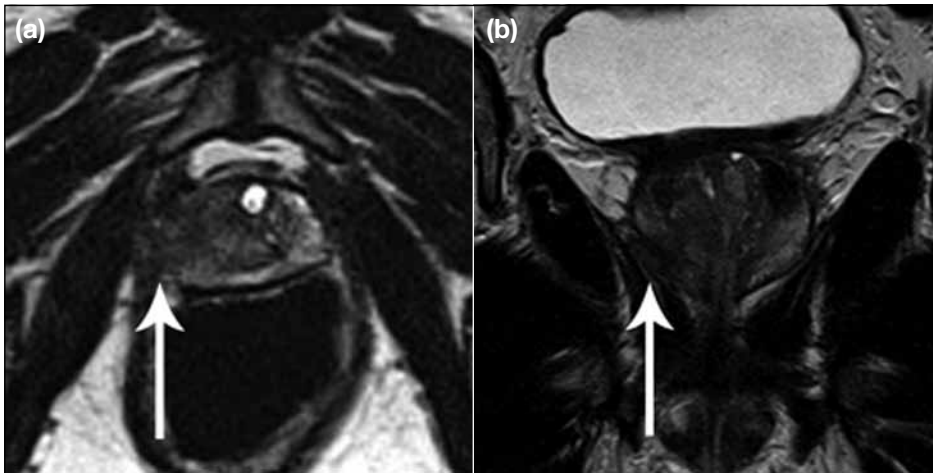


Figure 4. Magnetic resonance images show extracapsular extension of prostate cancer. (a) T2-weighted axial and (b) coronal images demonstrate low-signal-intensity tumour in the right peripheral zone with extension and interruption of the low-signal intensity prostatic capsule (arrows).

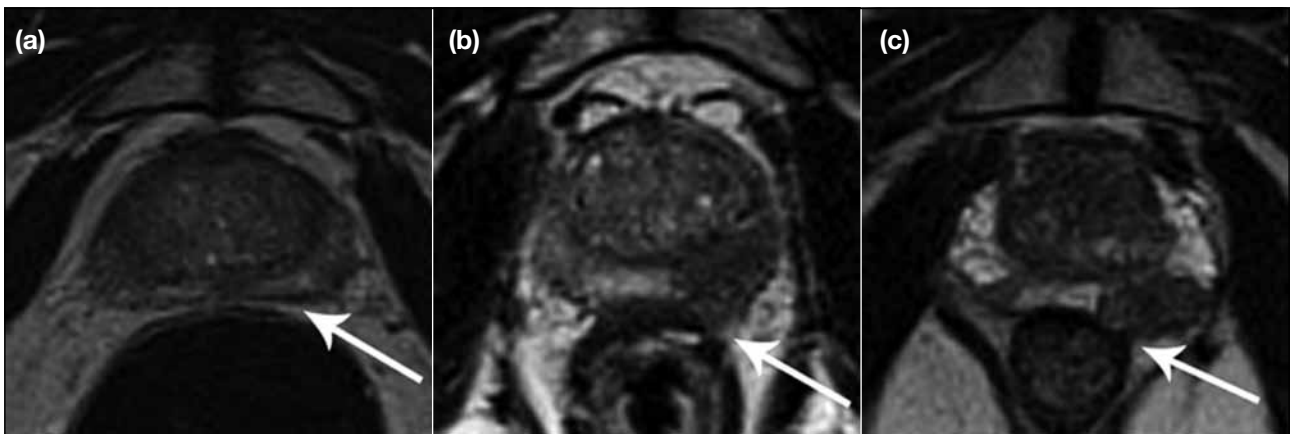


Figure 5. Axial T2-weighted magnetic resonance images of the prostate gland of three different patients demonstrate the (a) normal-shape rectoprostatic angle (arrow), (b) slightly blunted left rectoprostatic angle (arrow), and (c) marked blunting of the left rectoprostatic angle (arrow).

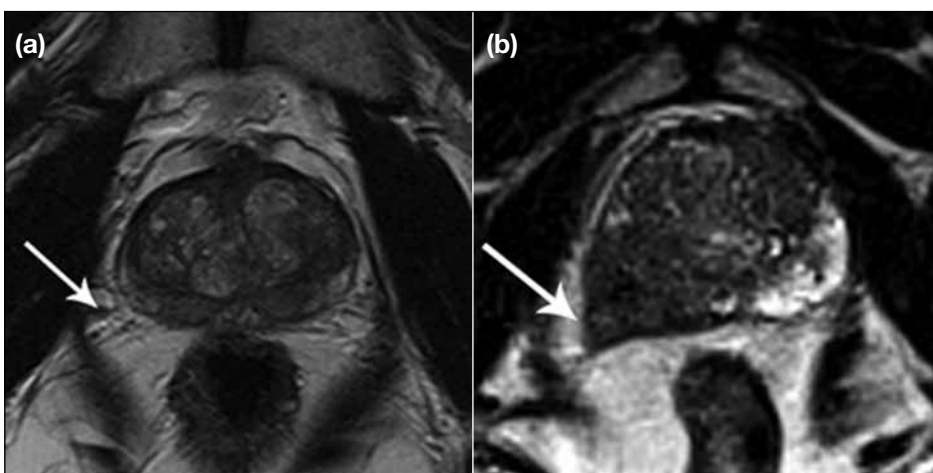


Figure 6. Axial T2-weighted magnetic resonance images show (a) normal appearance of the neurovascular bundle appearing as T2 low-signal 'dots' posterolateral to each side of the prostate gland (arrow), and (b) T2 low-signal tumour in the right posterior peripheral zone with invasion into the right neurovascular bundle (arrow). The hypointense neurovascular bundle is engulfed by the tumour and the T2 low-signal prostatic capsule is breached.



Figure 7. Axial T2-weighted magnetic resonance image shows T2 low-signal tumour in the right posterior peripheral zone. Focal bulging of the tumour is demonstrated (arrow). The T2 low-signal prostatic capsule is breached.

Magnetic Resonance Spectroscopy

MRS is a promising development in prostate cancer detection. A spectrograph is generated with peaks representing metabolite concentration within each voxel of data. Metabolites of interest include citrate and choline. MRS is able to demonstrate lower citrate levels and higher choline levels in prostate cancer compared with healthy prostate tissue (Figure 11). Performing MRS will usually add 15 to 20 minutes to the MRI time.²¹ The resulting spectral information can be overlaid onto the T2-weighted images for interpretation. In qualitative analysis, the spectra are visually compared. In quantitative analysis, a choline plus creatinine to citrate ratio is determined by software (Siemens NUMARIS/4). These ratios can be interpreted as a 5-point scale to assess the probability of malignancy (Table 4).¹⁹ MRS has been shown to increase the accuracy of the diagnosis, but it is not recommended to be performed alone.^{22,23} It has also been shown to be a valid tool for detecting recurrence and monitoring the therapeutic response.²⁴

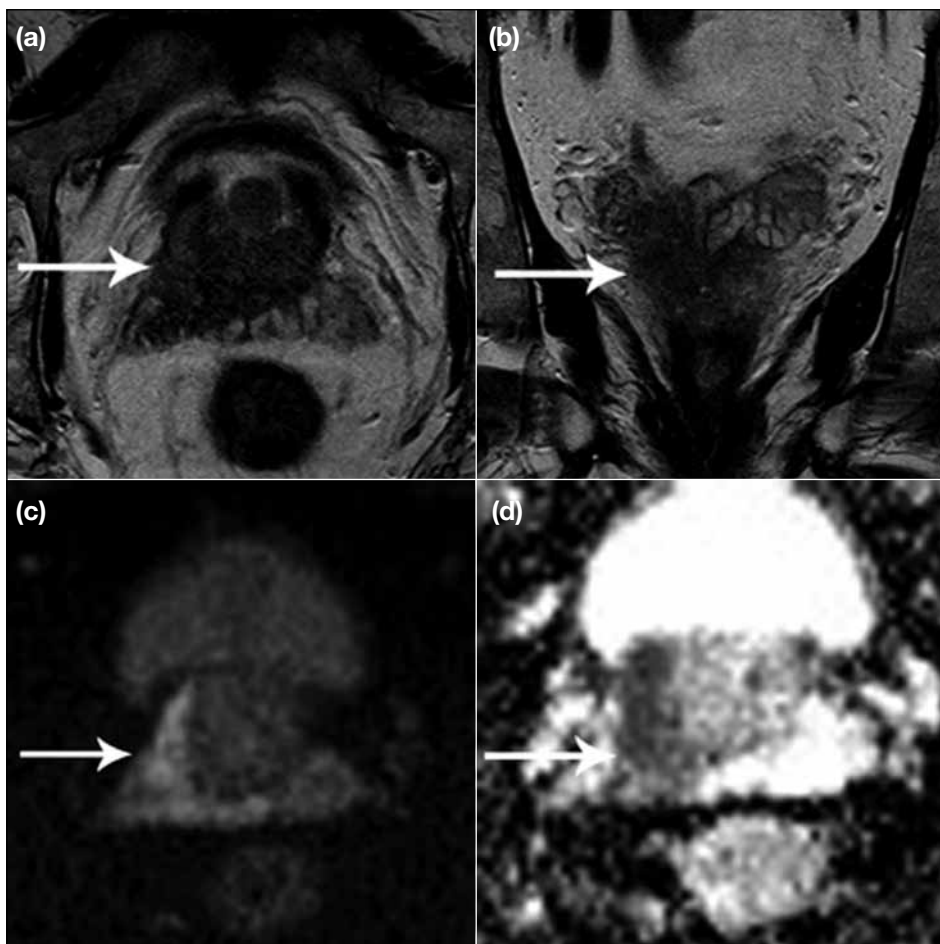


Figure 8. Magnetic resonance images of the prostate. (a) Axial and (b) coronal T2-weighted images show T2 low-signal tumour in the right posterior peripheral zone (arrows). The T2 low-signal tumour demonstrates invasion into the right seminal vesicle. The normal high-signal seminal vesicle is replaced by tumour and the normal convoluted architecture is lost. (c) Diffusion-weighted image and (d) apparent diffusion coefficient map of the same patient show an area of restricted diffusion extending posteriorly to the right seminal vesicle (arrows).

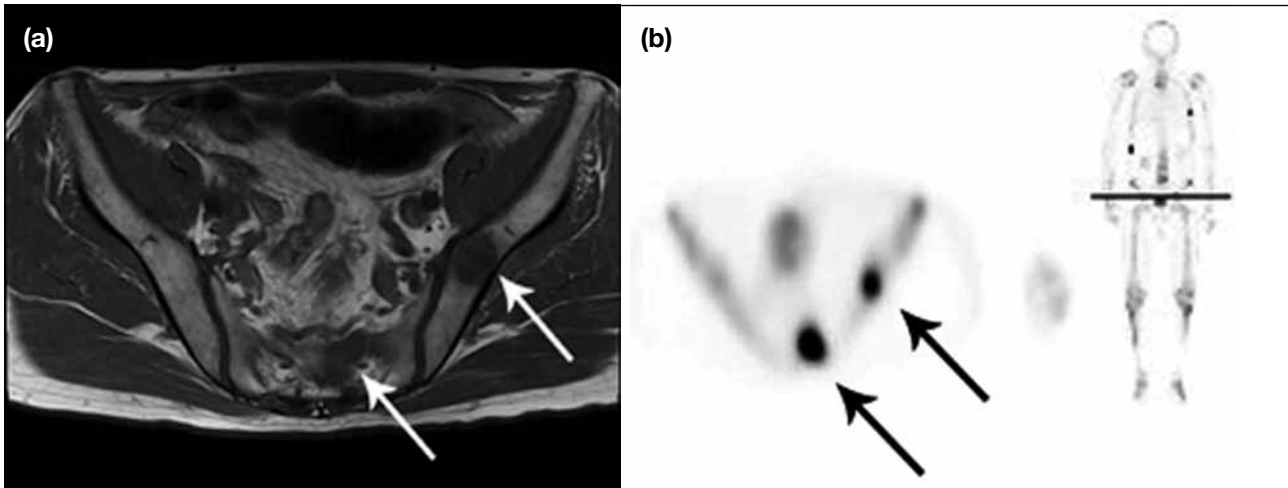


Figure 9. Magnetic resonance images of a 70-year-old man with rising prostate-specific antigen levels and a prostate mass. (a) T1-weighted large field-of-view image demonstrates low-signal-intensity lesions replacing the normal high-signal fatty bone marrow in the left ilium and left sacrum (white arrows). (b) Technetium^{99m}-methylene diphosphonate bone scan shows increased uptake (black arrows) in areas corresponding to the magnetic resonance imaging-detected abnormalities representing osseous metastases.

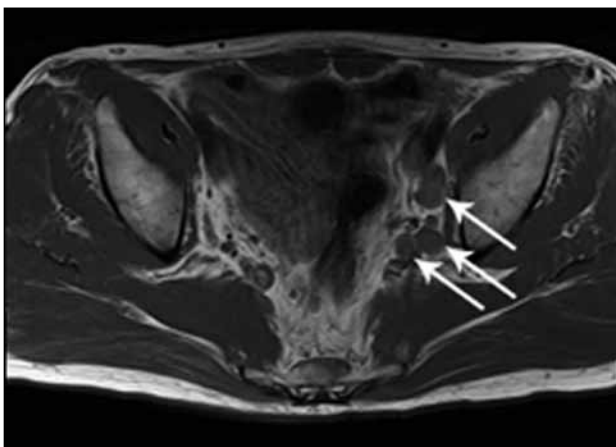


Figure 10. T1-weighted large field-of-view magnetic resonance image demonstrates enlarged left internal iliac lymph nodes (arrows) in a patient with known prostate cancer representing nodal metastasis.

Dynamic Contrast-enhanced Magnetic Resonance Imaging

DCE-MRI is a high-temporal-resolution imaging of the prostate after gadolinium administration. DCE-MRI is used to assess tumour vascularity. A series of 3D T1-weighted images are acquired after gadolinium administration to assess the degree of enhancement in the prostate. Interpretation of DCE-MRI can include qualitative, semi-quantitative, or quantitative

evaluation. In the qualitative method, visual assessment of the suspected cancer enhancement is used to look for early arterial enhancement. The quantitative method uses software packages (Siemens NUMARIS/4) and DCE-MRI data to produce parametric maps that can aid diagnosis. The semi-quantitative method uses relative enhancement curves, which can be calculated to reveal a type 1 curve (progressive enhancement over time), type 2 curve (plateau, no change in enhancement over time), or type 3 curve (early rapid enhancement followed by decreased enhancement). The type 3 curve is most suspicious of prostate malignancy, especially if there is a corresponding focal abnormality on other sequences.²⁵ Sensitivity and specificity can reach up to 76.5% and 89.5%, respectively, in patients with prior negative TRUS-guided prostate biopsy.²⁵ DCE-MRI has been shown to improve detection of post-prostatectomy and post-radiotherapy recurrences.²⁶⁻²⁸

CONCLUSION

Conventional MRI combined with DWI plays a major role in detection and staging of prostate cancer. Understanding the features of ECE and metastasis has potential implications for treatment and prognosis of the disease. Multiparametric imaging with DCE-MRI and MRS has an adjunctive role for selected cases or for detection of recurrence after surgery or radiotherapy.

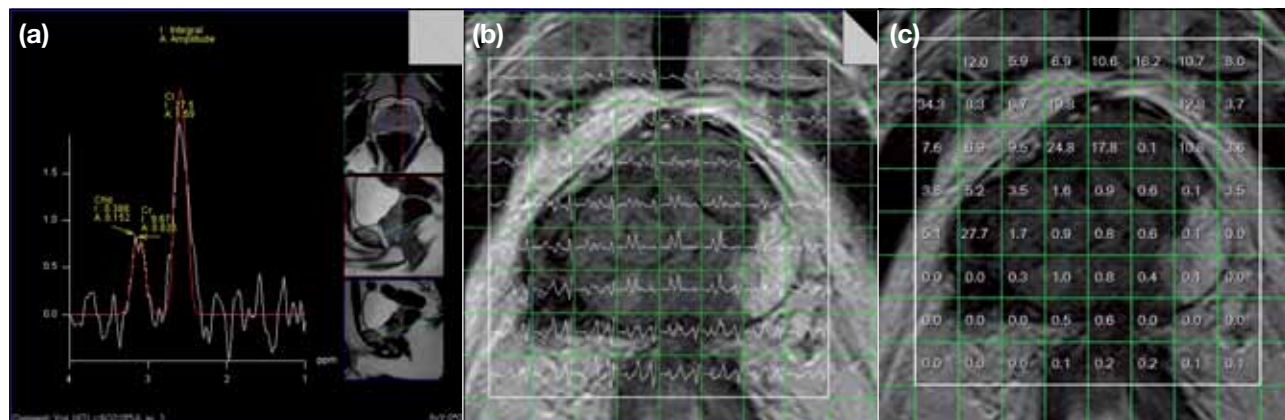


Figure 11. Magnetic resonance spectroscopy shows (a) a healthy prostate and (b) and (c) a prostate containing malignancy. In (a), citrate (Ci) is the predominant metabolite resonating at ~2.6 ppm. Choline (Cho) and creatinine (Cr) have overlapping spectra at 3.0-3.2 ppm and are read together as a summation of Cho and Cr peaks. The Cho and Cr peaks are much lower than the Ci peak. In (b), the spectra graph in the left lobe healthy prostate tissue resembles the spectra in (a), but shows suppressed Ci peak in the right lobe containing the prostate cancer. (c) A (Cho+Cr) to Ci ratio is generated and superimposed on the axial T2-weighted image showing elevated ratios in the area of the T2 low-signal tumour.

Table 4. European Association of Urology scoring system for choline plus creatinine: citrate ratio for different prostatic tissues.¹⁹

Rating	Peripheral zone	Central zone
1. Definitely benign	≤0.44	≤0.52
2. Probably benign	0.44-0.58	0.52-0.66
3. Possible malignant	0.58-0.72	0.66-0.80
4. Probably malignant	0.72-0.86	0.80-0.94
5. Definitely malignant	>0.86	>0.94

REFERENCES

1. Top ten cancers in 2012. Available from: www3.ha.org.hk/cancereg/statistics.html. Accessed Jan 2015.
2. Graham J, Kirkbride P, Cann K, Hasler E, Prettyjohns M. Prostate cancer: summary of updated NICE guidance. *BMJ*. 2014;348:f7524. [cross ref](#)
3. Claus FG, Hricak H, Hattery RR. Pretreatment evaluation of prostate cancer: role of MR imaging and 1H MR spectroscopy. *Radiographics*. 2004;24 Suppl 1:S167-80. [cross ref](#)
4. Boesen L, Chabanova E, Løgager V, Balslev I, Mikines K, Thomsen HS. Prostate cancer staging with extracapsular extension risk scoring using multiparametric MRI: a correlation with histopathology. *Eur Radiol*. 2014;25:1776-85. [cross ref](#)
5. Bloch BN, Furman-Haran E, Helbich TH, Lenkinski RE, Degani H, Kratzik C, et al. Prostate cancer: accurate determination of extracapsular extension with high-spatial-resolution dynamic contrast-enhanced and T2-weighted MR imaging — initial results. *Radiology*. 2007;245:176-85. [cross ref](#)
6. Porcaro AB, Borsato A, Romano M, Sava T, Ghimenton C, Migliorini F, et al. Accuracy of preoperative endo-rectal coil magnetic resonance imaging in detecting clinical under-staging of localized prostate cancer. *World J Urol*. 2013;31:1245-51. [cross ref](#)
7. McNeal JE. The zonal anatomy of the prostate. *Prostate*. 1981;2:35-

49. [cross ref](#)
8. Haider MA, van der Kwast TH, Tanguay J, Evans AJ, Hashmi AT, Lockwood G, et al. Combined T2-weighted and diffusion-weighted MRI for localization of prostate cancer. *AJR Am J Roentgenol*. 2007;189:323-8. [cross ref](#)
9. Tamada T, Sone T, Higashi H, Jo Y, Yamamoto A, Kanki A, et al. Prostate cancer detection in patients with total serum prostate-specific antigen levels of 4-10 ng/mL: diagnostic efficacy of diffusion-weighted imaging, dynamic contrast-enhanced MRI, and T2-weighted imaging. *AJR Am J Roentgenol*. 2011;197:664-70. [cross ref](#)
10. Oyen RH. Dynamic contrast-enhanced MRI of the prostate: Is this the way to proceed for characterization of prostatic carcinoma? *Eur Radiol*. 2003;13:921-4.
11. Hricak H, White S, Vigneron D, Kurhanewicz J, Kosco A, Levin D, et al. Carcinoma of the prostate gland: MR imaging with pelvic phased-array coils versus integrated endorectal — pelvic phased-array coils. *Radiology*. 1994;193:703-9. [cross ref](#)
12. Fütterer JJ, Scheenen TW, Huisman HJ, Klomp DW, van Dorsten FA, Hulsbergen-van de Kaa CA, et al. Initial experience of 3 tesla endorectal coil magnetic resonance imaging and 1H-spectroscopic imaging of the prostate. *Invest Radiol*. 2004;39:671-80. [cross ref](#)
13. Sosna J, Pedrosa I, Dewolf WC, Mahallati H, Lenkinski RE, Rofsky NM. MR imaging of the prostate at 3 Tesla: comparison of an external phased-array coil to imaging with an endorectal coil at 1.5 Tesla. *Acad Radiol*. 2004;11:857-62. [cross ref](#)
14. Ikonen S, Kivisaari L, Vehmas T, Tervahartiala P, Salo JO, Taari K, et al. Optimal timing of post-biopsy MR imaging of the prostate. *Acta Radiol*. 2001;42:70-3. [cross ref](#)
15. Ko YH, Song PH, Moon KH, Jung HC, Cheon J, Sung DJ. The optimal timing of post-prostate biopsy magnetic resonance imaging to guide nerve-sparing surgery. *Asian J Androl*. 2014;16:280-4. [cross ref](#)
16. Edge SB, Byrd DR, Compton CC, Fritz AG, Greene FL, Trotti A, et al. *Prostate*. *AJCC Cancer Staging Manual*. New York: Springer; 2010. p 457-68.
17. Kim CK, Park BK, Kim B. High-b-value diffusion-weighted

- imaging at 3 T to detect prostate cancer: comparisons between b values of 1,000 and 2,000 s/mm². *AJR Am J Roentgenol.* 2010;194:W33-7. [crossref](#)
18. Barentsz JO, Richenberg J, Clements R, Choyke P, Verma S, Villeirs G, et al. ESUR prostate MR guidelines 2012. *Eur Radiol.* 2012;22:746-57. [crossref](#)
 19. Heidenreich A, Aus G, Bolla M, Joniau S, Matveev VB, Schmid HP, et al. EAU guidelines on prostate cancer. *Eur Urol.* 2008;53:68-80. [crossref](#)
 20. Tokuda Y, Carlino LJ, Gopalan A, Tickoo SK, Kaag MG, Guillonnet B, et al. Prostate cancer topography and patterns of lymph node metastasis. *Am J Surg Pathol.* 2010;34:1862-7. [crossref](#)
 21. Verma S, Rajesh A, Fütterer JJ, Turkbey B, Scheenen TW, Pang Y, et al. Prostate MRI and 3D MR spectroscopy: how we do it. *AJR Am J Roentgenol.* 2010;194:1414-26. [crossref](#)
 22. Goeb K, Engehausen DG, Krause FS, Hollenbach HP, Niedobitek G, Buettner M, et al. MRI spectroscopy in screening of prostate cancer. *Anticancer Res.* 2007;27:687-93.
 23. Fütterer JJ, Heijmink SW, Scheenen TW, Veltman J, Huisman HJ, Vos P, et al. Prostate cancer localization with dynamic contrast-enhanced MR imaging and proton MR spectroscopic imaging. *Radiology.* 2006;241:449-58. [crossref](#)
 24. Pickett B, Kurhanewicz J, Coakley F, Shinohara K, Fein B, Roach M 3rd. Use of MRI and spectroscopy in evaluation of external beam radiotherapy for prostate cancer. *Int J Radiat Oncol Biol Phys.* 2004;60:1047-55. [crossref](#)
 25. Verma S, Turkbey B, Muradyan N, Rajesh A, Cornud F, Haider MA, et al. Overview of dynamic contrast-enhanced MRI in prostate cancer diagnosis and management. *AJR Am J Roentgenol.* 2012;198:1277-88. [crossref](#)
 26. Pasquier D, Hugentobler A, Masson P. Which imaging methods should be used prior to salvage radiotherapy after prostatectomy for prostate cancer? [in French]. *Cancer Radiother.* 2009;13:173-81. [crossref](#)
 27. Cirillo S, Petracchini M, Scotti L, Gallo T, Macera A, Bona MC, et al. Endorectal magnetic resonance imaging at 1.5 Tesla to assess local recurrence following radical prostatectomy using T2-weighted and contrast-enhanced imaging. *Eur Radiol.* 2009;19:761-9. [crossref](#)
 28. Haider MA, Chung P, Sweet J, Toi A, Jhaveri K, Ménard C, et al. Dynamic contrast-enhanced magnetic resonance imaging for localization of recurrent prostate cancer after external beam radiotherapy. *Int J Radiat Oncol Biol Phys.* 2008;70:425-30. [crossref](#)